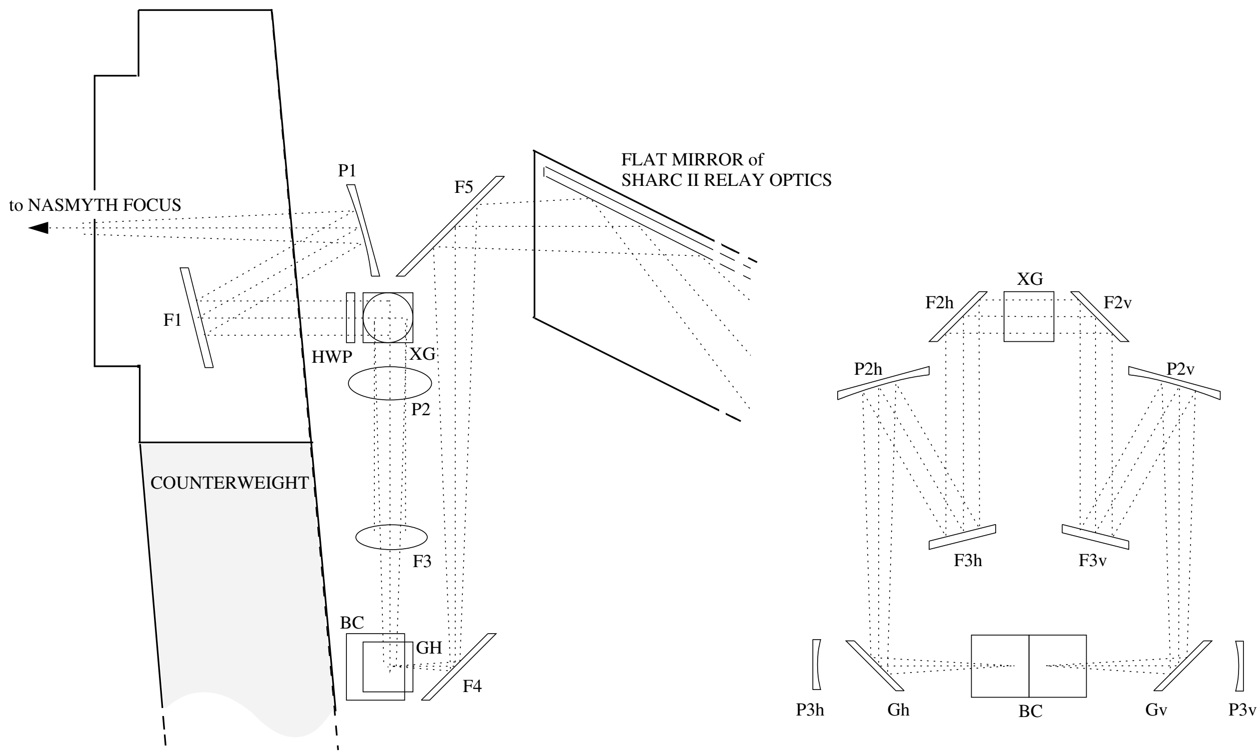

Figure 10: Two views of SHARP. Left: The expanding beam from the Nasmyth focus is reflected by paraboloid P1 and by flat F1, passes through the half-wave plate HWP, and reaches the crossed grid XG (Fig. 11). From XG, the vertical polarization component propagates into the plane of the paper while the horizontal component is directed towards the viewer. Right: View towards the Nasmyth focus. Vertical and horizontal components leaving the crossed grid undergo further reflections by mirrors and grids (F2v-F3v-P2v-Gv and F2h-F3h-P2h-Gh, respectively), ultimately bringing the components back together at the beam combiner BC which directs the recombined image towards the viewer. (BC consists of two mirrors joined at 90°, such that the reflective surfaces are analogous to the outside of a roof.) After reflection by BC, the two orthogonal polarizations are displaced laterally. The left view shows this reconstituted image being directed into the relay optics by flats F4 and F5. P1 and P2h (or P2v) form a pair of crossed paraboloids (Serabyn 1995). Paraboloids P3h and P3v ensure that for unused polarization components the time-reversed beams from SHARC-II are directed back into the cryostat, (e.g., via the paths F5-F4-BC-P3h-BC-F4-F5). SHARC-II is easily converted back to photometric mode by removing P1 and F5.

position (Hildebrand et al. 2000). SHARP collaborator C. Dowell will ensure that the SHARC-II data acquistion system software will be extended to include support for polarimetry (see letter of support from Dowell attached to Hildebrand proposal). The half-wave plate is controlled by an Ethernet Data Acquisition System (EDAS) that interfaces to a stepper motor indexer and an absolute encoder.

SHARP collaborator M. Houde, at the University of Western Ontario, is sharing the responsibility for developing data reduction software with U. Chicago postdoc J. Vaillancourt. (See letter from M. Houde attached to Novak proposal.) This Canadian participation in SHARP is funded entirely by Canadian sources.

SHARP data reduction algorithms will differ from those we have used with Hertz at the CSO. The degree of polarization is obtained by dividing the polarized flux (derived from differences of orthogonally polarized signals) by the total flux. For observations of faint sources, however, the denominator is often the sensitivity-limiting factor. The solution (Li et al. 2004)

Table 1: Specifications of SHARP

Central Wavelength	*350 μm*	*450 μm*[a]
Bandwidth $\Delta\lambda/\lambda_0$	0.13	0.10
Field of view of 12 pixel × 12 pixel array	$55'' \times 55''$	$55'' \times 55''$
Pixel size	$4.6'' \times 4.6''$	$4.6'' \times 4.6''$
Pixel size, measured in terms of (λ/D)	0.66 λ/D	0.52 λ/D
Angular resolution	$9''$	$11''$
Point source flux for $\sigma_P = 1\%$ in 5 hours[b]	2.7 Jy	1.5 Jy
Surface brightness for $\sigma_P = 1\%$ in 5 hours[b]	0.46 Jy per SHARP pixel[c]	0.26 Jy per SHARP pixel[c]
Max. separation of main and reference beams	$8'$	$8'$
Systematic errors, σ_P(sys.)	$\leq 0.2\%$	$\leq 0.2\%$

[a]all estimates of required flux for 450 μm band are ±20%
[b]assumes binning over 4 SHARP pixels, which is approximately one resolution element
[c]one SHARP pixel = $4.6'' \times 4.6'' = 21$ arcsec^2

Table 2: Predicted Efficiency of SHARP

Source of Inefficiency	*Magnitude of Inefficiency*	*Basis for Estimate*
absorption in half-wave plate (HWP)	5–10%	Murray et al. 1992
imperfect A/R coating on HWP	1% (× 2 surfaces)	experience with SPARO
absorption by mirrors and grids	0.5% (× 10 reflections)	theory of classical skin effect
Ruze losses (curved mirrors only)	3% (× 2 mirrors)	5 μm r.m.s. surface error
loss due to grid imperfections	5% (total loss)	dominated by split element of crossed grid
HWP modulation inefficiency	2%	Novak et al. 1989
diffraction losses due to vignetting	∼0%	ZEEMAX-EE modeling (see §3.1)
imperfect termination of unused polarization components	0.5 – 5.0%	assumes termination to 30 K (BE and indep. photon statistics)
net efficiency of SHARP, relative to SHARC-II	∼73.5%	product of (1.0−inefficiency) for all terms above

for HAWC/SOFIA based on the SHARP concept. For these far-IR wavelengths, reflective retarders such as those described by Chuss et al. (2004b) and Siringo et al. (2004) will be required because crystals (at room temperature) are too lossy. It should also be feasible to use the SHARP concept to convert new large-format cameras currently being constructed for the LMT and SPT into sensitive polarimeters.

The PolKa collaboration at the Max Planck Institute (MPI) in Bonn is pursuing another approach to the problem (Siringo et al. 2004). Instead of rapidly chopping the secondary, they use a rapidly spinning reflective half-wave plate, with a polarizing grid installed between the spinning retarder and the camera. The technique removes much of the sky noise, but suffers from systematic errors due to polarization of background by off-axis reflections (Siringo et al. 2004). The MPI technique is expected to be implemented with the LaBoca 800 μm camera at APEX. For telescopes lacking a chopping secondary, the MPI technique is especially attractive, but it remains unclear whether it can achieve background limited polarimetric performance.

4 Management

As discussed, the organization of the technical effort will be led collaboratively by Hilde-